Evaluation and comparison of a new DOTA and DTPA-bombesin agonist in vitro and in vivo in low and high GRPR expressing prostate and breast tumor models

Priscilla B. Pujatti [a,b,*], Julie M. Foster [a], Ciara Finucane [c], Chantelle D. Hudson [a], Jerome C. Burnet [d], Kerly F.M. Pasqualoto [e], Jair Mengatti [b], Stephen J. Mather [a], Elaine B. de Araújo [b], Jane K. Sosabowski [a]

[a] Centre for Molecular Oncology, Barts Cancer Institute, Queen Mary University of London, London EC1M 6BQ, United Kingdom
[b] Nuclear and Energy Research Institute (IPEN), University of Sao Paulo, Sao Paulo, Brazil
[c] InviCRO LLC, 27 Drydock Ave, Boston, MA 02210, United States
[d] Biospace Lab, 13 rue Georges Auric, 75011 Paris, France
[e] Laboratory of Biochemistry and Biphysics, Butantan Institute, Sao Paulo, Brazil

HIGHLIGHTS

- A new DOTA or DTPA-bombesin analog was evaluated in GRPR expressing tumor models.
- The peptide could bind specifically only to T-47D, LNCaP and PC-3 cells in vitro.
- Saturation binding assays showed that the affinity of DOTA and DTPA peptide is similar.
- Greater internalization, but not efflux, of the DOTA-peptide was observed.
- Both peptides could target PC-3 and LNCaP tumors in vivo.

ARTICLE INFO

ABSTRACT

We evaluated and compared a new bombesin analog [Tyr–Gly$_5$, Nle^{14}]-BBN(6–14) conjugated to DOTA or DTPA and radiolabeled with In-111 in low and high GRPR expressing tumor models. Both peptides were radiolabeled with high radiochemical purity and specific activity. In vitro assays on T-47D, LNCaP and PC-3 cells showed that the affinity of peptides is similar and a higher binding and internalization of DOTA-peptide to PC-3 cells was observed. Both peptides could target PC-3 and LNCaP tumors in vivo and both tumor types could be visualized by microSPECT/CT.

© 2014 Elsevier Ltd. All rights reserved.

1. Introduction

Radiolabeled receptor-binding peptides have emerged as an important class of radiopharmaceuticals for tumor diagnosis and therapy Laverman et al. (2012). The basis of the use of peptides in tumor targeting is the overexpression of their receptors on tumor cell membranes Reubi (2003). One peptide that has become a focus of interest is bombesin (BBN), a 14-amino acid peptide originally isolated from the skin of a European frog. Bombesin binds with high affinity to gastrin releasing peptide receptors (GRPR). These receptors are known to be overexpressed in various human tumors and tumor cell lines including breast, prostate, small cell lung, pancreatic (Smith et al., 2005; J.C. Reubi et al., 2002), urinary tract (Fleischmann et al., 2009) and ovarian cancers (Fleischmann et al., 2009). In the field of breast and prostate cancers, C. Reubi et al. (2002) detected GRPR in high density in epithelial mammary, ductal and lobular breast carcinomas and also in primary and invasive prostate carcinomas (Markwalder and Reubi, 1999). More recently, Beer et al. (2012) showed that primary prostate carcinomas and metastases express high numbers of

* Corresponding author. Present address: Nuclear Medicine Section, National Cancer Institute, Praça da Cruz Vermelha, 23, Centro, Rio de Janeiro, RJ, Brazil.
E-mail address: pujatti.pb@gmail.com (P.B. Pujatti).

GRPR. These findings and others have made targeting of GRPR an attractive model for development of site-directed diagnostic/therapeutic agents based upon radiolabeled bombesin analogs.

Several radiolabeled bombesin agonists have already been described as promising tools for prostate and breast tumor diagnosis and therapy (Liu et al., 2009; Wild et al., 2011; Lantry et al., 2006; Lane et al., 2010; de Visser et al., 2007; Maina et al., 2005). In general, these ligands are analogs of full-length BBN(1–14) or are truncated analogs based on the C-terminal sequence, BBN(7–14), which confers receptor binding affinity. Most bombesin analogs are high affinity GRPR binding peptides, but a group of analogs based on a universal bombesin ligand (Mantey et al., 1997; Pradhan et al., 1998) additionally bind to the other two mammalian BBN receptor subtypes i.e. BB1 (the neuromedin B receptor) and the orphan receptor, BB3. These peptides have been termed the pan-bombesin ligands (Zhang et al., 2004; Schuhmacher et al., 2005). Also, recent developments are focusing on bombesin antagonists. The data suggest that the GRP antagonists may be superior targeting agents to GRP receptor agonists, because of their lower accumulation in the pancreas, liver and intestines. In addition, the antagonists have the potential to have fewer side-effects compared to the agonists (Gourni et al., 2014; Jamous et al., 2014).

Previous reports showed the advantages of using trivalent radiometals as important components for producing radiolabeled BBN analogs. Lanthanide or lanthanide-like radiometals are readily available, possess similar radiolabeling chemistries in aqueous solution, can produce high specific activity radiopeptides and offer a wide range of nuclear properties to choose from. Furthermore, kinetically inert conjugates with high in vivo stability can be obtained using multidentate chelators (Smith et al., 2005).

In the case of the bombesin analogs, both the macrocyclic agent DOTA- (1,4,7,10-tetraazacyclododecane-1,4,7,10-tetraacetic acid) and the acyclic agent DTPA (diethylenetriaminepentaacetic acid) have been extensively used as chelators for labeling with radiometals and enable high specific activity labeling with ^{111}In. DTPA-conjugated peptides are preferable for ^{111}In-labeling because of the possibility of labeling at lower temperatures and usually higher specific activities are achieved (Schroeder et al., 2010; Breeman et al., 2002). On the other hand, in some cases, DOTA-peptides have afforded higher stability in vitro and in vivo (Zhang et al., 2004).

Recent studies of radiolabeled bombesin analogs have shown that small changes to analog structure, conjugated chelator and/or radioisotope can significantly influence their pharmacokinetics and biodistribution (Gourni et al., 2014; Jamous et al., 2014; Liu et al., 2013; Marsouvanidis et al., 2013; Okarvi and Jammaz 2012). Considering this, we designed a bombesin agonist *in silico* starting from the structure of bombesin and we constructed lipophilicity maps of structure-modified bombesin derivatives. The hydrophobic interactions of the molecules with the receptor, the transfer mechanisms through biological membranes, as well as the toxicity of the molecule are, in part, determined by their lipophilicity. The maps describe graphically how lipophilicity is distributed over the different groups of a molecule, based on the theoretical octanol–water partition coefficient of each group (Csizmadia et al., 1997). Based on this, we selected a derivative less

lipophilic than the parent peptide or some others of the analogs described in the literature: [Tyr–Gly$_5$, Nle^{14}]-BBN(6–14). It was hoped that this would increase the rate of blood clearance, reducing any non-target mediated uptake without significantly compromising tumor uptake. In addition, Met^{14} was replaced by the synthetic amino acid norleucine in order to avoid oxidation during the radiolabeling process. We evaluate and compare the potential of this bombesin analog – conjugated either to DOTA or DTPA (Table 1) and radiolabeled with In-111 for targeting and imaging different GRP receptor expressing prostate and breast tumor cells. The comparison was performed using different in vitro methods, to detect and analyze peptides targeted to GRPR positive cells, and in vivo in animal models of human GRPR positive tumors. Some in vivo studies were performed, as a comparison using the same mouse model and tumor cell lines, with the bombesin derivative BZH3. This bombesin derivative has been described previously and consists of a PEG$_2$ spacer between DOTA and the [Tyr^6, βAla^{12}, Thi^{13}, Nle^{14}]BBN(7–14) sequence, which confers to this analog one of the highest tumor and pancreatic uptake among the analogs studied (Schuhmacher et al., 2005).

2. Materials and methods

2.1. Chemicals

DOTA-[Tyr–Gly$_5$, Nle^{14}]-BBN(6–14)(DOTA-BEYG$_5$N) and DTPA-[Tyr–Gly$_5$, Nle^{14}]-BBN(6–14) (DTPA-BEYG$_5$N) were purchased from Anaspec (USA). Identity and purity were confirmed by matrix-assisted laser desorption/ionization mass spectroscopy (MALDI-MS) and reverse-phase high performance liquid chromatography (RP-HPLC).

BZH3 (Schuhmacher et al., 2005) was kindly provided by Prof. Dr. H Mäecke, University Hospital Freiburg, Germany. The following reagents were supplied from different sources: 2-(*N*-morpholino)ethanesulfonic acid (MES)**,** ammonium acetate, sodium azide, ethylenediaminetetraacetic acid (EDTA) and bovine serum albumin (BSA) from Sigma-Aldrich Co. (USA), trifluoroacetic acid (TFA) from Fluka (USA); RPMI 1640, DMEM, trypsin-EDTA and fetal bovine serum (FBS) from PAA (Austria); acetonitrile, acetic acid and sodium hydroxide from Fisher Scientific (UK); ^{111}InCl$_3$in 0.05 M HCl from Covidien (Netherlands). Reagents for Western Blot were purchased from National Diagnosis (UK). All reagents were of analytical grade and acetonitrile and trifluoroacetic acid were HPLC grade.

2.2. Analytical methods

2.2.1. Instant thin layer chromatography (ITLC)

Instant thin-layer chromatography (ITLC) was performed using iTLC-SG (Varian, Canada) and the following 2 solvent systems: 50 mM EDTA in 0.1 M ammonium acetate, pH 5.5, and 3.5% (v/v) ammonia/methanol, 1:1. In the EDTA and ammonium acetate system, ^{111}In-peptide remains at the origin (Rf=0) and ^{111}In-EDTA elutes to the solvent front (Rf=1). In the ammonia and methanol system, ^{111}In-peptide and ^{111}In-EDTA both have an Rf of 1 and any

Table 1
Amino acid sequences of bombesin (BBN) and derivatives.

Peptide	Chelator	Spacer	Amino acid sequence													
			1	2	3	4	5	6	7	8	9	10	11	12	13	14
BBN	–		pGlu	Gln	Arg	Leu	Gly	Asn	Gln	Trp	Ala	Val	Gly	His	Leu	Met
YG$_5$N	**DOTA or DTPA**	Tyr–Gly$_5$						Asn	Gln	Trp	Ala	Val	Gly	His	Leu	Nle
BZH3	**DOTA**	PEG$_2$						Tyr	Gln	Trp	Ala	Val	Gly	βAla	Thi	Nle

colloidal material present in the reaction mixture remains at the origin.

2.2.2. Reversed phase high performance liquid chromatography (RP-HPLC)

Radiochemical purity and stability analyses were performed using a Beckman System Gold 128 solvent module and a 166 UV detector module (monitoring at 280 nm) combined with a GABi Star radiochemical detector (Raytest, GmbH). Compounds were separated on a 5 μm Jupiter 300 column (250 × 4.6 mm i.d., Phenomenex), with the following conditions: solvent A, 0.1% trifluoroacetic acid (TFA) in water; solvent B, 0.1% TFA in acetonitrile; and gradient, 0% B for 2 min, changing to 60% B over 20 min, then to 100% B over 5 min and back to 0% B over 5 min (flow rate, 1 mL/min).

2.3. Cell culture

Human prostate grade IV adenocarcinoma (PC-3) and human breast adenocarcinoma (MDA-MB-231) cell lines (Cancer Research UK Cell Services, UK) were maintained in DMEM supplemented with 10% FBS. Human prostate carcinoma (LNCaP), human breast primary ductal carcinoma (BT-474) and human metastatic ductal carcinoma (T-47D) (Cancer Research UK Cell Services, UK) were maintained in RPMI supplemented with 4 mM L-glutamine and 10% FBS. Cells were kept in humidified air containing 5% CO_2 at 37 °C. The cells were grown up to 80% confluency, harvested by trypsinization and resuspended or plated according to each experiment.

2.4. Animal models

GRPR-positive xenografts were induced by subcutaneous injection of PC-3 (4×10^6/mouse) or LNCaP cells (5×10^6/mouse) in 0.2 mL of a mixture of PBS (phosphate buffered saline solution) and Matrigel (BD Biosciences, USA) 1:1 v/v to the left flank of 6-week old male beige SCID or SCID mice (Charles River Laboratories, UK). Animals were used 15–21 days later when the tumors had grown to around 5 mm in diameter.

2.5. Radiolabeling of DOTA and DTPA peptides with ^{111}In

To a 1.5 mL polypropylene vial was added 20–100 μL of $^{111}InCl_3$ (15–80 MBq) in 0.05 M HCl, 1 M MES buffer (pH 5.5) (one fifth the volume of $^{111}InCl_3$) and 2.0–10 μL of peptide (1 mg/mL in 0.4 M acetate buffer, pH 4.5). The solution was heated at 93 °C (DOTA-BEYG$_5$N and BZH3) or 25 °C (DTPA-BEYG$_5$N) for 10 min before the addition of 0.1 M ethylenediaminetetraacetic acid (EDTA) (5 mM in the reaction mixture). The solutions were diluted with PBS, and the radiochemical purity was determined using ITLC and RP-HPLC, as described earlier.

2.6. Theoretical partition coefficient (log P)

Theoretical partition coefficient of bombesin derivatives was calculated using Marvin Sketh 5.0 software (ChemAxon, EUA) by the method Weighted (Viswanadhan et al., 1989) with equal weights of VG, and PHYS KLOP methods and 0.1 M of Cl^-, Na^+ and K^+. This method calculates the partition coefficient by the sum of the partition coefficient of the groups that form the molecule.

2.7. In vitro studies

2.7.1. Assessment of GRP receptor expression

The expression of GRPR by PC-3 and LNCap human prostate cancer cells and BT-474, MDA-MB-231 and T-47D human breast cancer cells was investigated by Western blot. The cells were cultured in 15 cm dishes. When a monolayer of cells had formed, they were washed with ice-non-radioactive PBS, scraped into 1 mL of non-radioactive PBS and centrifuged at 1000g for 5 min. The cells were then lysed in buffer containing 50 mM Tris–HCl (pH 7.5), 150 mM sodium chloride, 1% Triton X-100, 1% deoxycholate, 1% sodium azide, 1 mM ethyleneglycolteeraacetic acid, 0.4 M EDTA, 1.5 μg/ml aprotinin, 1.5 μg/ml leupeptin, 1 mM phenylmethylsulfonylfluoride and 0.2 mM sodium vanadate (Sigma-Aldrich, USA). The lysate was kept on ice for 20 min and then centrifuged at 10000g for 10 min. Protein concentration was measured using the DC-Protein Assay kit (Biorad Laboratories, USA). The expression of GRPR receptors in the samples was analyzed by sodium dodecyl sulfate/polyacrylamide gel electrophoresis (SDS-PAGE) and Western blotting. The proteins were fractionated using 10% polyacrylamide gel, transferred to nitrocellulose membranes and incubated overnight at 4 °C with 1 μg/ml anti-GRP receptor antibody (Abcam, UK), followed by anti-rabbit immunoglobulin G-horseradish peroxidase conjugate (Dako, Denmark). The membrane was washed three times for 10 min with washing solution (50 mM Tris–HCl (pH 8.0), 2 mM $CaCl_2$, 80 mM sodium chloride, 0.05% Tween 20 and 0.02% sodium azide). The blot was incubated with enhanced chemiluminescence detection (GE Healthcare, UK) reagent and exposed to Kodak XAR film. After revealing the film, the gel was washed three times for 10 min with washing solution and incubated overnight at 4 °C with 1 μg/ml anti-tubulin receptor antibody (Dako, Denmark), followed by anti-rabbit immunoglobulin G-horseradish peroxidase conjugate (Dako, Denmark), in order to determine the amount of protein in each sample. After three washes of 10 min each, the blot was incubated with enhanced chemiluminescence detection (GE Healthcare, UK) reagent and exposed to Kodak XAR film. The intensity of the GRPR and tubulin bands was compared.

2.7.2. Receptor binding assays

Cell binding assays were performed with ^{111}In-DOTA-BEYG$_5$N on PC-3, LNCaP, BT-474, MDA-MB-231 and T-47D cells. Radiolabeling was performed as described previously to a specific activity of 100 MBq/nmol and diluted with culture media containing 1% FBS to give a 4×10^5 cpm/mL solution. The non-radioactive peptide (10,000 nM in culture media containing 1% v/v FBS) was used as the competitor. The assay was performed by adding different number of cells (0.125, 0.25, 0.5 and 1.0×10^6 in 0.5 mL of culture media containing 1% v/v FBS) to a 1.5-mL polypropylene vial, followed by 250 μL of either culture media (1% FBS) (to measure total binding) or 250 μL of competitor (to measure non-specific binding) in triplicate and 250 μL of the diluted labeled peptide. The tubes were incubated at 20 °C for 1.5 h, centrifuged at 5000g for 5 min, washed twice with 1 mL PBS/1% BSA and counted. The percentages of total binding, specific binding and non-specific binding versus cell number was plotted using GraphPad Prism software (version 5.0).

Saturation binding assays with ^{111}In-DOTA-BEYG$_5$N and ^{111}In-DTPA-BEYG$_5$N were performed on whole adherent PC-3, LNCaP and T-47D cells, which had been seeded in 6-well plates (2.5×10^5/well) and incubated as before for 24 h. Radiolabeling was performed as described previously to specific activity of 1.3 MBq/nmol. Then a 2-fold molar excess of stable isotope $InCl_3$ was added and the mixture reacted for a further 5 min before addition of EDTA dilution with PBS to give a 4000 nM solution. The assay was performed as previously described (Sosabowski et al., 2009). Briefly, the cells were incubated at 20 °C for 1.5 h with increasing concentrations (0.1–40 nM) of radioligand both with and without competitor (10,000 nM non-radioactive DOTA- or DTPA-peptide) in triplicate in the presence of 0.1% (w/v) sodium azide to minimize internalization. After removal of the incubation mixture, the cells were washed at 0 °C, lysed with 1 M NaOH and the lysates

removed and counted in the gamma counter. Standards of the total activity added to the wells were also counted. The protein content of three wells was determined using the DC Protein Assay kit (Biorad Laboratories). Dissociation constant (K_d) and maximum numbers of binding sites (Bmax) were calculated using nonlinear regression (GraphPad Prism software version 5.0).

2.7.3. Internalization and efflux

PC-3 cells were seeded in 6-well plates (2.5×10^5/well) and maintained as before for 48 h prior to the assay. The medium was removed and the cells were washed twice with ice-non-radioactive internalization medium (DMEM supplemented with 1% v/v FBS), and then 1.2 mL of internalization medium was added to each well, followed by the addition of 150 µL of ^{111}In-DOTA-BEYG$_5$N or ^{111}In-DTPA-BEYG$_5$N in 1% (w/v) BSA/PBS buffer and either 150 µL of 1% (w/v) BSA/PBS alone (to measure total counts) or 150 µL of 10 µM competitor (either DOTA-BEYG$_5$N or DTPA-BEYG$_5$N) in 1% (w/v) BSA/PBS to measure nonspecific binding. The wells corresponding to total binding and nonspecific binding were pipetted in triplicate for each time point of 10 and 30 min and 1 and 2 h of incubation at 37 °C. Incubation was stopped at each time point by removal of the medium and washing the cells twice with ice-non-radioactive internalization medium. The cells were then treated with 1 mL of 20 mM sodium acetate pH 5.0 in HBSS for 10 min, followed by a quick wash, and the acid wash was collected and placed in counting tubes. For internalization analysis, the cells were then lysed with 1 M NaOH, which was removed to counting tubes after 15 min, along with 2×1 mL of PBS wash (the internalized fraction). Additionally, the protein content of three wells was determined using the DC Protein Assay kit (Biorad Laboratories) after washing them twice with 1 mL of PBS. After counting, the specific internalized mean values were calculated and represented as a percentage of total activity added.

For efflux analysis, the assay was performed as described for 60 min, followed by the acid wash to remove the surface-bound radiopeptide. Then, 1.5 mL of internalization medium was added to each well and the plates were incubated at 37 °C for 10, 30, 60 or 120 min. After each time point, the media was collected to counting tubes, along with 2×1 mL PBS/1% BSA washes (externalized fraction), and the cells were then lysed with 1 M NaOH, which was removed to counting tubes after 15 min, along with 2×1 mL of PBS wash (the internalized fraction). After counting the tubes, the externalized mean values were calculated and represented as a percentage of total activity internalized.

2.7.4. Stability in mouse plasma

Animal studies were carried out in accordance with the UK Animals (Scientific Procedures) Act 1986. BALB/c mice (Charles River Laboratories, UK) were anesthetized with 2% isoflurane gas and 0.5 L/min oxygen and blood was collected by cardiac puncture into an EDTA tube to prevent clotting. Subsequently, samples were centrifuged for 5 min, 3000g at 4 °C to separate the plasma. Then, ^{111}In-DOTA-BEYG$_5$N or ^{111}In-DTPA-BEYG$_5$N (20 MBq) was added to 1 mL of mouse plasma and incubated for 15 min, 1, 4 or 24 h at 37 °C. After each time point, an aliquot of each sample was collected in duplicate, the proteins were precipitated with ethanol (serum:ethanol 1:1) followed by centrifuging for 10 min at 10,000g. The supernatant containing the radiolabeled peptide was analyzed by HPLC and the percentage of intact radiolabeled peptide was determined (% intact peptide of each sample per time point).

2.8. In vivo studies

2.8.1. In vivo stability assays

Analysis of in vivo stability in blood was performed in non-tumor-bearing male BALB/c mice (Charles River Laboratories, UK)

injected i.v. via the tail vein with 1 nmol ^{111}In-DOTA-BEYG$_5$N or ^{111}In-DTPA-BEYG$_5$N (20 MBq) in a volume of 200 µL of PBS. After 5 and 15 min p.i., the animals were anesthetized with 2% isoflurane gas and 0.5 L/min oxygen and blood was collected by cardiac puncture into an EDTA tube to prevent clotting and put on ice. Subsequently, samples were centrifuged for 5 min, 3000g at 4 °C, after which the supernatant was collected, proteins precipitated with ethanol (serum:ethanol 1:1) and centrifuged for 10 min at 10,000g. The supernatant was analyzed by HPLC (Schroeder et al., 2010) and the percentage of intact radiolabeled peptide was determined (% intact peptide of each mouse per time point). For each time point, three animals were used.

In vivo stability studies in mouse tissues were performed as previously described (Ocak et al., 2011). SCID mice were injected with 4×10^6 PC-3 cells subcutaneously in the left flank and the animals used 15–21 days after injection, when tumors reached approximately 5 mm diameter. ^{111}In-DOTA-BEYG$_5$N, ^{111}In-DTPA-BEYG$_5$N and ^{111}In-BZH3 (13–15 MBq, 0.13 nmol, 0.2 mL of PBS) were injected i.v. via the tail vein in PC-3 tumor-bearing mice ($n=2$). At 1 h p.i., the mice were sacrificed and the tumor, pancreas and kidneys were placed in 0.5 mL of ice-non-radioactive 20 mM HEPES buffer pH 7.3 and homogenized using an Ultra-Turrax T8 homogenator for 5 min. Samples were precipitated with ACN (1:1), vortexed and then centrifuged (10,000g, 5 min). The supernatant was transferred into a 1.5 mL polypropylene vial tube and recentrifuged (10,000g, 5 min). The supernatants were evaporated to half of the volume, diluted with double distilled water (1:1) and analyzed via RP-HPLC to determine the percentage of intact peptide.

2.8.2. Biodistribution studies in xenografted mice

PC-3 or LNCap tumor-bearing (male SCID) mice ($n=3$ per peptide) were injected i.v. with 200 µL (13 MBq, 0.13 nmol) of either ^{111}In-labeled BEYG$_5$N peptide or the bombesin derivative ^{111}In-BZH3 (Schuhmacher et al., 2005). The mice were anesthetized with 2% isoflurane gas and 0.5 L/min oxygen and sacrificed 4 h p.i. and the blood, tumor, pancreas, kidneys, heart, stomach, spleen, intestine, liver, lung, and muscle were sampled; each sample was weighed and counted in a γ-counter (LKB Compugamma) along with dose standards and the percentage of injected dose per gram (% ID/g) of tissue was calculated for each tissue type.

2.8.3. In vivo blocking studies

In order to evaluate whether binding of bombesin analogs to PC-3 cells in vivo is specific, we carried out blocking studies with ^{111}In-DOTA-BEYG$_5$N in PC-3 tumor bearing male SCID mice.

Groups of three animals were injected with either 0.03 nmol of ^{111}In-DOTA-BEYG$_5$N (2 MBq) alone or with 25 nmol of non-radioactive peptide and 0.03 nmol of the radiolabeled analog (2 MBq). After 4 h, the mice were anesthetized with 2% isoflurane gas and 0.5 L/min oxygen and sacrificed 4 h p.i. and the organs were sampled; each sample was weighed and counted in a γ-counter (LKB Compugamma) along with dose standards and the percentage of injected dose per gram (% ID/g) of tissue was calculated for each tissue type.

2.8.4. Nano-SPECT imaging and quantification

For imaging studies, ^{111}In-DOTA-BEYG$_5$N, ^{111}In-DTPA-BEYG$_5$N and ^{111}In-BZH3 (13–15 MBq, 0.13 nmol) were injected via the tail vein in PC-3 and LNCap tumor-bearing mice. At 1 and 4 h p.i., the mice were anesthetized with 2% isoflurane gas and 0.5 L/min oxygen and whole body SPECT images obtained (45 min each) using a NanoSPECT/CT four-head camera (Bioscan Inc, Washington DC, USA) fitted with 2 mm pinhole collimators in helical scanning mode (20 projections, 45 min scan) and CT images with a 45-kVP X-ray source. After scanning at 4 h, the animals were sacrificed

and the tissues and organs dissected out and counted in a gamma counter. Images were reconstructed in a 256×256 matrix using proprietary Bioscan software and fused using PMOD (Mediso). The uptake in tumor and muscle was quantified using In vivo Scope (Bioscan). The % ID/g was also calculated using the weight of the tissue obtained after dissection. All SPECT-quantified activities were corrected for decay and were compared to the ex vivo biodistribution values.

2.8.5. Statistical analysis

The results are expressed as mean $\pm$ SE for in vitro assays and mean$+$SD for animal experiments. Statistical analysis was performed using GraphPad PRISM 5.0 (USA) software using Student´s t-test with two-tailed distribution for paired data and One-way ANOVA analysis of variance for grouped data. Differences at the 95% confidence level ($p < 0.05$) were considered significant.

3. Results

3.1. Radiolabeling of DOTA and DTPA peptide with ^{111}In

ITLC and RP-HPLC analysis showed that the all the peptides could be radiolabeled with high radiochemical purity ($> 97\%$) and a maximum specific activity of 100 MBq/nmol or 174 MBq/nmol was obtained for ^{111}In-DOTA-BEYG$_5$N (and also for ^{111}In-BZH3) and ^{111}In-DTPA-BEYG$_5$N, respectively.

3.2. Partition coefficient determination

Partition coefficient results showed that the new bombesin analogs should show low lipophilicity in comparison to the PEG-containing BZH3. The theoretical partition coefficients of DTPA-BEYG$_5$N, DOTA-BEYG$_5$N and BZH3 were $-9,97$, $-10,01$ and $-3,12$, respectively.

3.3. In vitro studies

3.3.1. Assessment of GRP receptor expression

Two human prostate cancer cell lines and three human breast cancer cell lines were examined for GRPR expression by immunoblotting. The results obtained for the 50 kDa band, which corresponds to GRPR, are shown in Figs. 1 and 2. All cell lines express the receptor, although BT-474 and T-47D only show low amounts. The highest expression levels of GRPR were seen in PC-3 and LNCaP human prostate adenocarcinoma cell lines.

3.3.2. Receptor binding assays

The ability of the new bombesin derivatives to bind GRPR expressed by the five cell lines was investigated with ^{111}In-DOTA-BEYG$_5$N using an increasing number of tumor cells in the absence and presence of competitor (excess non-radioactive

Fig. 1. GRPR western blot demonstrated that the analyzed human prostate and breast cancer cell lines express different GRPR levels. Equal amounts of tubulin were loaded onto the gel as a control of the amount of protein in each sample. These results are representative of three experiments.

peptide) to measure total and non- specific binding, respectively. The results are shown in Fig. 2. ^{111}In-DOTA-BEYG$_5$N showed highest specific binding to PC-3 and LNCap prostate cancer, confirming the high expression of GRPR on those cells, as demonstrated by Western blot. Also, ^{111}In-DOTA-BEYG$_5$N showed low, but specific binding to T-47D breast cancer cells. However, although MDA-MB-231 and BT-474 have shown low amounts of GRPR in Western blot relative to their respective tubulin controls, binding of ^{111}In-DOTA-BEYG$_5$N was low and non-specific.

As ^{111}In-DOTA-BEYG$_5$N bound specifically to PC-3, LNCaP and T-47D cells, these cells were used in saturation binding assays to compare the affinities of ^{111}In-DOTA-BEYG$_5$N and ^{111}In-DTPA-BEYG$_5$N for the receptors (Kd), as well as the number receptors per cell (Bmax) and the results are shown in Table 2. Assays carried out with both peptides showed that the Bmax of the T-47D cells was significantly lower than that of the PC-3 and LNCap cells. The average number of receptors was measured as being two-fold higher in PC-3 cells than in LNCaP cells and T47-D express more than 10-fold fewer receptors than do PC-3 cells. There was no difference in the affinity (Kd) of the DOTA-BEYG$_5$N and the DTPA-BEYG$_5$N for the receptor.

3.3.3. Internalization and efflux

The receptor-mediated internalization of ^{111}In-DOTA-BEYG$_5$N and ^{111}In-DTPA-BEYG$_5$N was studied in adherent human prostate PC-3 cells, as this cell line had the highest receptor expression out of all the studied cells (Fig. 1). The internalized fraction of both radiopeptides reached a plateau of 90–95% of total bound activity after 30 min of incubation (not shown). The percentage internalized of total added activity per mg of total cell protein, is higher for ^{111}In-DOTA-BEYG$_5$N than ^{111}In-DTPA-BEYG$_5$N, especially up 60 min of incubation (Fig. 3a). These results correlate with the saturation binding assays (Table 2), which demonstrate that ^{111}In-DTPA-BEYG$_5$N recognizes fewer binding sites (lower Bmax) on PC-3 cells than does the DOTA-bombesin derivative.

An assay was carried out in order to determine the rate of peptide externalization after 1 h internalization and the results are shown in Fig. 3b. After 2 h of incubation at 37 °C approximately 60% of internalized activity had become externalized. There was however no significant difference between the externalization ratios of^{111}In-DOTA-BEYG$_5$N and ^{111}In-DTPA-BEYG$_5$N.

3.4. In vitro stability in mouse plasma

After incubation of labeled peptides in mouse plasma for increasing periods of time, HPLC analysis was used to calculate the percentage of intact radiopeptide at each time point The results suggest some metabolic degradation of peptides by mouse serum from 4 h onwards (see Table 3) after which ^{111}In-DOTA-BEYG$_5$N stability was higher than that of ^{111}In-DTPA-BEYG$_5$N.

3.5. In vivo studies

3.5.1. In vivo stability assays

In vivo stability analysis in blood (Table 4) showed that both ^{111}In-DOTA-BEYG$_5$N and ^{111}In-DTPA-BEYG$_5$N have low in vivo stability and no intact radiopeptide was detected at 15 min post injection. However, the stability of ^{111}In-DOTA-BEYG$_5$N was higher than that of the DTPA peptide as evidenced by a higher amount of intact peptide detected in blood at 5 min p.i. Analysis of total radioactivity in serum and that bound to plasma proteins showed that 85–90% of total activity was extracted from the serum after the precipitation procedure (data not shown).

Analysis of radiopeptide stability in tumor, pancreas and kidneys 1 h p.i. showed that ^{111}In-DOTA-BEYG$_5$N and ^{111}In-BZH3 are comparably stable in tumor (approximately 70% intact radiopeptide), followed by ^{111}In-DTPA-BEYG$_5$N (20% of intact peptide)
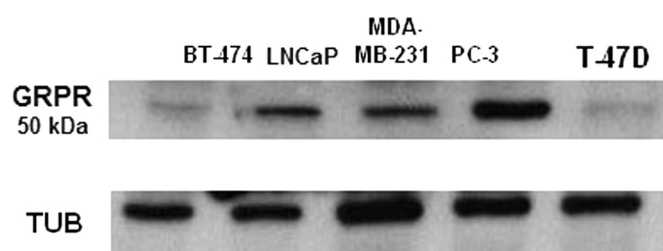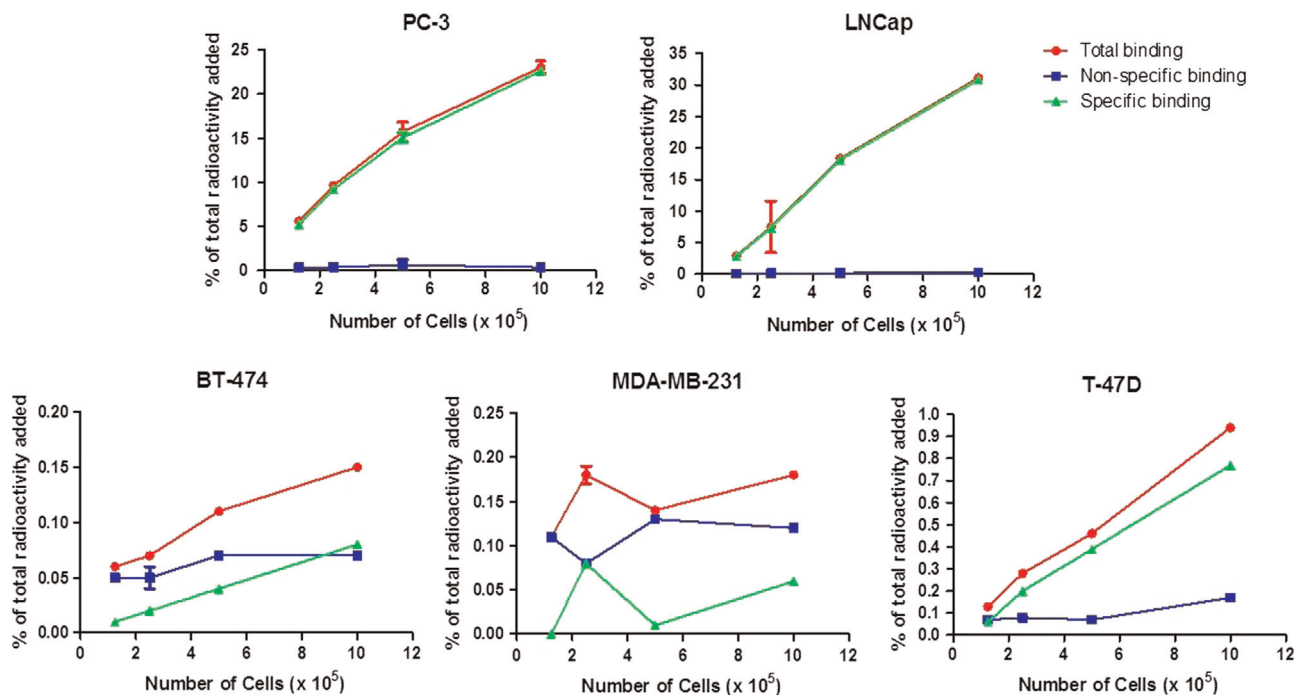
Fig. 2. Binding of ^{111}In-DOTA-BEYG$_5$N to human prostate (PC-3 and LNCap) and breast cancer (BT-474, MDA-MB-231 and T-47D) cell lines. The binding to PC-3 and LNCap cells is high and specific while the binding to BT-474 and MDA-MB-231 is low and non-specific. The results are representative of three experiments.

Table 2
Saturation binding of ^{111}In-DOTA-BEYG$_5$N and ^{111}In-DTPA-BEYG$_5$N to different tumor cell lines analyzed by non-linear regression. These results are the mean of 3 separate saturation binding assays $\pm$ SE.

Cell line	PC-3	LNCap	T-47D
^{111}In-DOTA-BEYG$_5$N			
Bmax (fmol/mg)	550.6 ± 37.9	231.6 ± 36.5	61.52 ± 12.4
Bmax (recep/cell) ($\times 10^5$)	6.08 ± 1.6	2.79 ± 0.5	0.38 ± 0.09
Kd (nM)	1.29 ± 0.4	1.77 ± 0.5	3.16 ± 1.3
^{111}In-DTPA-BEYG$_5$N			
Bmax (fmol/mg)	355.10 ± 13.0	140.60 ± 5.0	70.78 ± 11.9
Bmax (recep/cell) ($\times 10^5$)	3.22 ± 0.7	1.55 ± 0.2	0.4 ± 0.04
Kd (nM)	1.26 ± 0.2	1.78 ± 0.3	3.45 ± 0.4

(Table 5). ^{111}In-DOTA-BEYG$_5$N was also more stable in pancreas than ^{111}In-DTPA-BEYG$_5$N and ^{111}In-BZH3 and the stability of the three radiopeptides in kidneys was very low and variable, suggesting that they are not excreted intact in the urine.

3.5.2. Biodistribution studies in xenografted mice

Results of biodistribution studies of ^{111}In-DOTA-BEYG$_5$N, ^{111}In-DTPA-BEYG$_5$N and ^{111}In-BZH3 in various tissues and in PC-3 and LNCap tumors at 4 h p.i. are summarized in Tables 6 and 7 as percentage of injected radioactive dose per gram of tissue (% ID/g). In PC-3 tumors the highest uptake was obtained with ^{111}In-BZH3 ($1.40 \pm 0.2\%$ ID/g), followed by ^{111}In-DOTA-BEYG$_5$N ($0.81 \pm 0.1\%$ ID/g) and ^{111}In-DTPA-BEYG$_5$N ($0.49 \pm 0.1\%$ ID/g) ($p < 0.05$). However, the tumor-to-muscle ratios were similar for the three peptides. In addition, the uptake of the three radiopeptides in LNCap tumors was comparable and not significantly different (1.33 ± 0.1, 1.05 ± 0.1 and $1.50 \pm 0.4\%$ ID/g for ^{111}In-DOTA-BEYG$_5$N, ^{111}In-DTPA-BEYG$_5$N and ^{111}In-BZH3, respectively), although the tumor to muscle ratio for ^{111}In-DOTA-BEYG$_5$N was significantly higher than for the other two radiopeptides.

^{111}In-BZH3 showed the highest uptake in the GRPR expressing pancreas (4–5 fold higher) and large intestine (2-fold higher) than
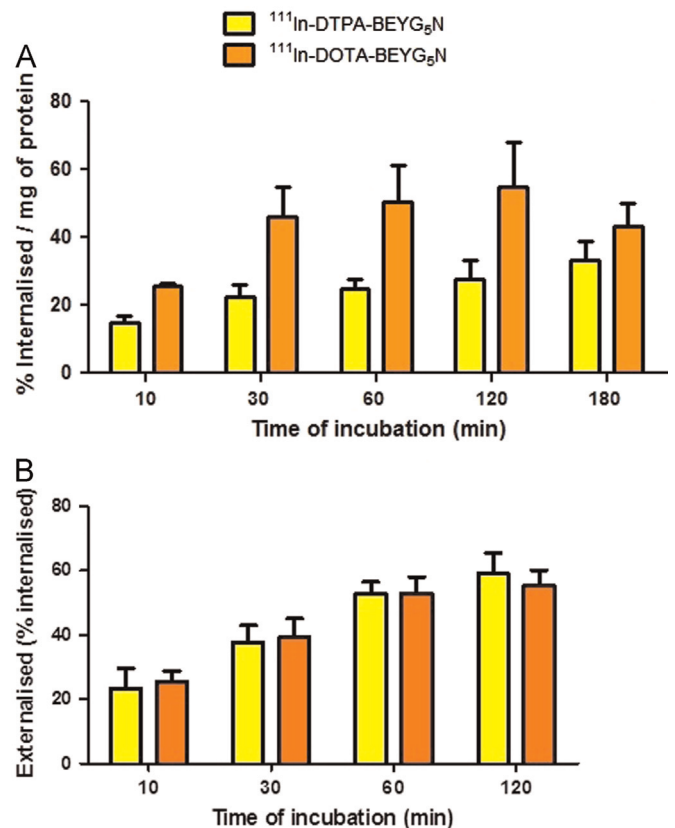
Fig. 3. Internalization (A) and efflux (B) of ^{111}In-DOTA-BEYG$_5$N and ^{111}In-DTPA-BEYG$_5$N by PC-3 cells at different incubation times at 37 °C. The results are the mean of three separate experiments $\pm$ SE.

^{111}In-DOTA-BEYG$_5$N and ^{111}In-DTPA-BEYG$_5$N, where colon is the GRPR-expressing segment. For all three peptides, apart from receptor-expressing tissues, only kidney was measured to have any

Table 3

Intact radiopeptide (%), determined by HPLC, after incubation in mouse plasma at increasing time points. The results represent two different experiments (Expt).

	Intact peptide (%) determined by HPLC			
	^{111}In-DOTA-BEYG$_5$N		^{111}In-DTPA-BEYG$_5$N	
	Expt 1	Expt 2	Expt 1	Expt 2
15 min	98.68	95.01	96.95	95.07
1 h	95.15	94.46	94.24	91.46
4 h	92.29	78.20	74.87	67.19
24 h	47.55	27.20	14.55	11.72

Table 4

In vivo stability at 5 and 15 min post i.v. injection of 2 nmol (20 MBq) of ^{111}In-DOTA-BEYG$_5$N and ^{111}In-DTPA-BEYG$_5$N in healthy BALB/c mice. Results are presented as intact peptide as a percentage of total injected.

	^{111}In-DOTA-BEYG$_5$N		^{111}In-DTPA-BEYG$_5$N	
	5 min	15 min	5 min	15 min
Mouse 1	18.79	0	0	0
Mouse 2	15.08	0	5.90	0
Mouse 3	3.82	0	5.85	0

Table 5

Intact peptide (%) present in tumor, pancreas and kidneys 1 h p.i. of ^{111}In-DOTA-BEYG$_5$N, ^{111}In-DTPA-BEYG$_5$N or ^{111}In-BZH3 after i.v. injection in male PC-3 tumor-bearing beige SCID mice.

Organ/ peptide	PC-3 tumor		Pancreas		Kidneys	
	Mouse 1	Mouse 2	Mouse 1	Mouse 2	Mouse 1	Mouse 2
^{111}In-DOTA-BEYG$_5$N	78.9	75.8	26.8	44.8	19.9	0.0
^{111}In-DTPA-BEYG$_5$N	30.7	14.0	10.5	3.0	15.9	0.0
^{111}In-BZH3	76.4	66.1	5.5	7.8	0.0	2.0

Table 6

Biodistribution studies of ^{111}In-DOTA-BEYG$_5$N, ^{111}In-DTPA-BEYG$_5$N and ^{111}In-BZH3 in PC-3 tumor bearing male beige SCID mice 4 h p.i. of 0.13 nmol (13 MBq) of each peptide ($n=3$). The mice were anesthetized with 2% isoflurane gas and 0.5 L/min oxygen before sacrificing. The results are expressed in percentage of injected dose per gram of tissue (% ID/g).

	^{111}In-DOTA-BEYG$_5$N	^{111}In-DTPA-BEYG$_5$N	^{111}In-BZH3
Tumor	0.81 ± 0.1	0.49 ± 0.1	1.40 ± 0.2
Small intestine	0.46 ± 0.02	0.33 ± 0.1	1.13 ± 0.1
Large intestine	3.38 ± 1.0	1.80 ± 0.4	4.51 ± 0.4
Pancreas	2.47 ± 0.5	2.00 ± 0.7	8.37 ± 1.5
Spleen	0.34 ± 0.1	0.22 ± 0.1	0.46 ± 0.03
Stomach	0.36 ± 0.2	0.33 ± 0.1	0.50 ± 0.2
Kidney	2.48 ± 0.6	2.68 ± 0.4	2.87 ± 0.7
Liver	0.14 ± 0.01	0.30 ± 0.03	0.69 ± 0.1
Heart	0.04 ± 0.01	0.05 ± 0.01	0.07 ± 0.02
Lungs	0.08 ± 0.02	0.09 ± 0.03	0.15 ± 0.01
Blood	0.03 ± 0.01	0.07 ± 0.02	0.06 ± 0.01
Muscle	0.14 ± 0.2	0.09 ± 0.1	0.26 ± 0.2
Tumor:blood	28.2 ± 21.4	7.07 ± 1.6	26.00 ± 9.6
Tumor:pancreas	0.27 ± 0.1	0.26 ± 0.1	0.17 ± 0.01
Tumor:kidneys	0.29 ± 0.1	0.18 ± 0.0	0.50 ± 0.1
Tumor:liver	4.62 ± 2.0	2.31 ± 1.4	2.04 ± 0.3
Tumor:muscle	23.00 ± 10.5	9.10 ± 8.5	20.54 ± 13.4

Table 7

Biodistribution studies of ^{111}In-DOTA-BEYG$_5$N, ^{111}In-DTPA-BEYG$_5$N and ^{111}In-BZH3 in LNCaP tumor-bearing male SCID mice 4 h p.i. of 0.13 nmol (13 MBq) of each peptide ($n=3$). The mice were anesthetized with 2% isoflurane gas and 0.5 L/min oxygen before sacrificing. The results are expressed as percentage of injected dose per gram of tissue (% ID/g).

	^{111}In-DOTA-BEYG$_5$N	^{111}In-DTPA-BEYG$_5$N	^{111}In-BZH3
Tumor	1.33 ± 0.1	1.05 ± 0.1	1.50 ± 0.4
Small intestine	0.59 ± 0.2	0.21 ± 0.01	0.79 ± 0.3
Large intestine	2.02 ± 0.9	1.54 ± 0.1	4.11 ± 0.9
Pancreas	2.64 ± 0.6	1.68 ± 0.5	11.14 ± 3.1
Spleen	0.27 ± 0.1	0.29 ± 0.2	0.35 ± 0.3
Stomach	0.22 ± 0.1	0.10 ± 0.01	0.50 ± 0.4
Kidney	3.27 ± 0.2	3.43 ± 0.1	2.30 ± 0.2
Liver	0.14 ± 0.01	0.18 ± 0.01	0.74 ± 0.01
Heart	0.03 ± 0.01	0.07 ± 0.02	0.04 ± 0.01
Lungs	0.07 ± 0.02	0.13 ± 0.02	0.14 ± 0.1
Blood	0.02 ± 0.01	0.07 ± 0.02	0.05 ± 0.02
Muscle	0.01 ± 0.01	0.04 ± 0.01	0.03 ± 0.01
Tumor:blood	86.9 ± 3.9	7.07 ± 1.6	33.04 ± 15.4
Tumor:pancreas	0.52 ± 0.1	0.26 ± 0.1	0.14 ± 0.0
Tumor:kidneys	0.41 ± 0.1	0.31 ± 0.01	0.66 ± 0.2
Tumor:liver	9.27 ± 0.6	5.77 ± 0.8	2.05 ± 0.6
Tumor:muscle	104.87 ± 13.5	22.32 ± 19.5	44.88 ± 18.0

3.6. In vivo blocking studies of ^{111}In-DOTA-BEYG$_5$N

In accordance with the in vitro binding studies, the binding of the peptide to the receptor in vivo appears to be specific. Blocking studies performed with ^{111}In-DOTA-BEYG$_5$N showed that co-administration of 850-fold molar excess of unlabeled DOTA-BEYG$_5$N had the effect of reducing uptake in GRPR expressing tissues: by approximately 60% in tumor ($p < 0.05$) and by approximately 90% in pancreas ($p < 0.001$). Uptake in other tissues was not significantly reduced (Fig. 4).

3.6.1. Nano-SPECT imaging and quantification

Imaging was performed on PC-3 and LNCaP tumor-bearing mice at 1 and 4 h post injection of ^{111}In-DOTA-BEYG$_5$N, ^{111}In-DTPA-BEYG$_5$N or ^{111}In-BZH3. Representative examples of the images obtained at 4 h are shown in Fig. 5. Significant uptake is visible in the tumors, abdominal region (pancreas and large intestines) and kidneys, with the tumor uptake of the ^{111}In-DOTA-BEYG$_5$N being clearly greater than that of ^{111}In-DTPA-BEYG$_5$N and comparable to that of ^{111}In-BZH3, especially in LNCaP tumor.

Results from quantification of image VOI's using In vivo Scope software (Bioscan, Inc.) are shown in Table 8. PC-3 tumor uptake 1 h p.i. was higher for ^{111}In-DOTA-BEYG$_5$N when compared to ^{111}In-DTPA-BEYG$_5$N ($p=0.013$), but not statistically different to that of ^{111}In-BZH3. Tumor uptake was comparable for ^{111}In-BZH3
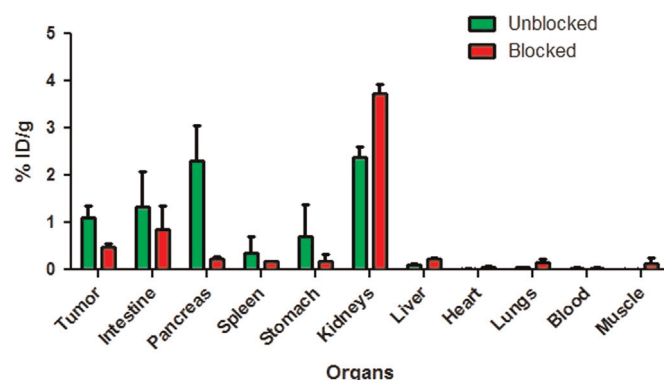
Fig. 4. Biodistribution of ^{111}In-DOTA-BEYG$_5$N (0.03 nmol) in the presence (25 nmol) and absence of the non-radioactive peptide (blocker) ($n=3$).

significant levels of radioactivity which, along with low liver and blood, indicates fast blood clearance and rapid excretion via the renal pathway.
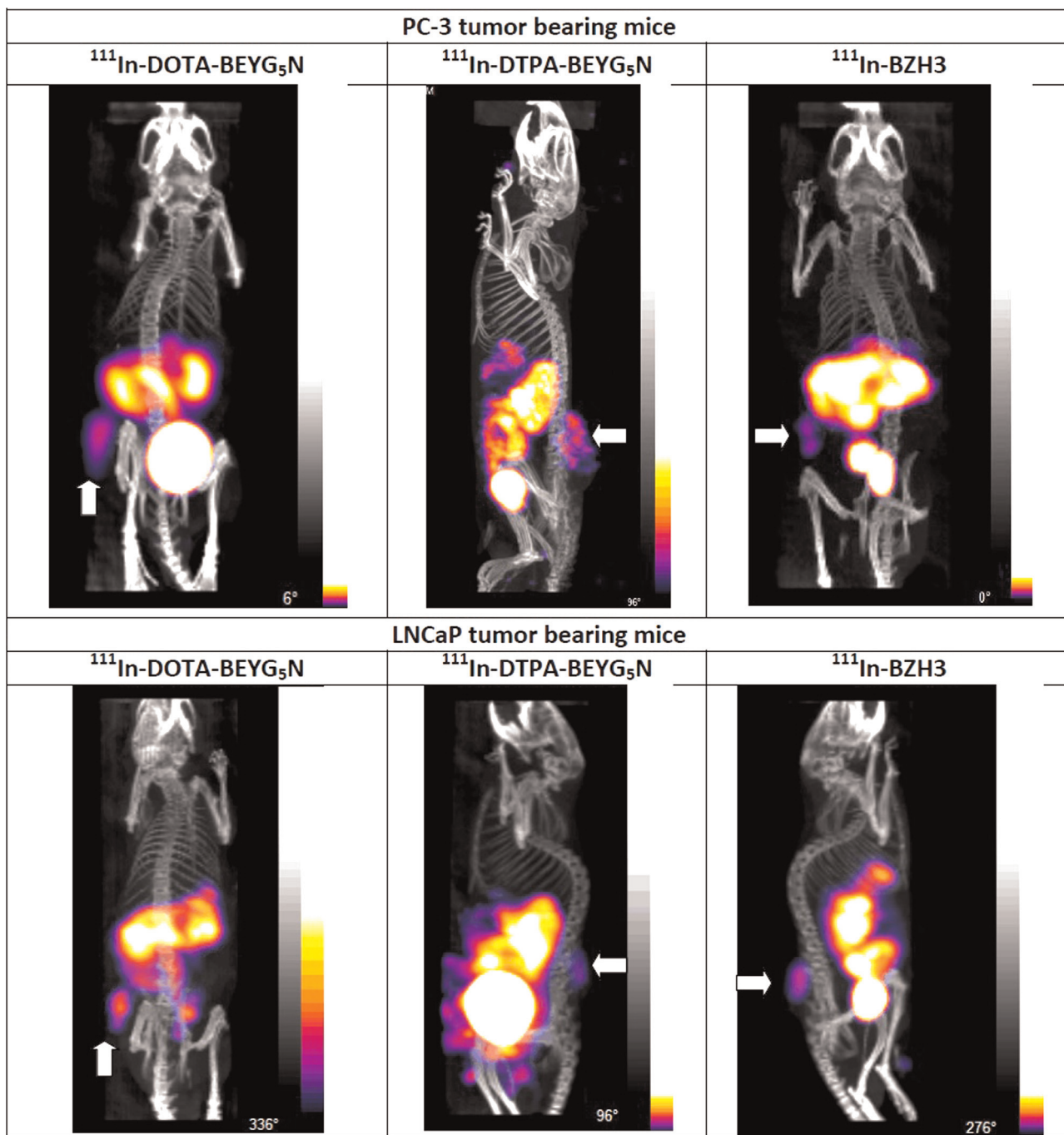
Fig. 5. NanoSPECT/CT images of PC-3 and LNCaP prostate tumor-bearing mice after 4 h p.i. of ^{111}In-DOTA-BEYG5N, ^{111}In-DTPA-BEYG5N and ^{111}In-BZH3. The white arrows indicate tumor position.

and ^{111}In-DTPA-BEYG5N at 1 h p.i and for the three radiopeptides at 4 h p.i. However, the superior visualization of PC-3 tumor with ^{111}In-DOTA-BEYG5N can be explained by its higher tumor to background (muscle) ratio. Although no difference was found when comparing the PC-3 tumor-to-muscle ratios of the three peptides 1 h p.i., this ratio was significantly higher for

Table 8

Quantification of tumor uptake by SPECT imaging (InVivoScope software, Bioscan, Inc.). The uptake in tumor and muscle was quantified using CT as a guide ($n=3$).

Radiopeptide	^{111}In-DOTA-BEYG5N		^{111}In-DTPA-BEYG5N		^{111}In-BZH3	
Time p.i.	1 h	4 h	1 h	4 h	1 h	4 h
% ID/g in PC-3 tumor	3.1 ± 0.2	1.1 ± 0.4	2.2 ± 0.1	1.2 ± 0.1	2.5 ± 1.0	1.1 ± 0.1
PC-3 tumor:muscle	14.2 ± 6.3	31.0 ± 3.4	28.4 ± 15.4	21.1 ± 2.8	22.3 ± 11.4	16.3 ± 2.9
% ID/g in LNCaP tumor	1.3 ± 0.2	1.0 ± 0.3	1.6 ± 0.6	0.8 ± 0.1	2.1 ± 0.3	1.3 ± 0.6
LNCaP tumor:muscle	31.8 ± 12.9	61.0 ± 26.3	14.0 ± 3.5	23.4 ± 10.0	20.2 ± 6.4	32.6 ± 6.6

^{111}In-DOTA-BEYG$_5$N when compared to that of ^{111}In-DTPA-BEYG$_5$N ($p=0.041$) and ^{111}In-BZH3 ($p=0.015$) at 4 h. This result differs from the biodistribution data, which demonstrated no differences among the tumor to muscle ratios of the three radiopeptides, as shown in Table 6.

For LNCaP tumor, ^{111}In-BZH3 uptake was higher than ^{111}In-DOTA-BEYG$_5$N ($p=0.019$) and comparable to that o f^{111}In-DTPA-BEYG$_5$N 1 h p.i. However at 4 h, the difference was not statistically significant for tumor uptake or tumor to muscle ratios at 1 and 4 h p.i. of the three radiopeptides.

4. Discussion

As new radiometals have emerged as potential candidates for radiolabeling peptides and antibodies for imaging and therapy, the choice of chelator has become increasingly important. Although the ligand is the most important factor in determining the properties of the radiomolecule, the chelator can directly influence its stability and in vivo behavior (Zhang et al., 2004; Fani et al., 2011). While in general, ^{111}In-DOTA peptides have tended to show superior in vivo characteristics in comparison to ^{111}In-DTPA radiolabeled compound (Schuhmacher et al., 2005), Zhang et al. (2004) showed the opposite to be true with an almost 2-fold higher tumor uptake at 4 h for the ^{111}In-DTPA BZH1 compound than that seen for the otherwise identical ^{111}In-DOTA analog (BZH2). Therefore the superiority of the In-DOTA complex over the In-DTPA complex in vivo cannot be assumed. In this study we applied different in vitro and in vivo methods to compare the ability of a new ^{111}In-labeled DOTA and DTPA bombesin analog to target low and high GRPR-expressing tumor cells. Due to large variations seen for the same peptides in vivo from lab to lab as has previously been shown in a study comparing 5 different bombesin analogs (Schroeder et al., 2010), for our in vivo work we also studied the BZH3 pan-bombesin analog (Schuhmacher et al., 2005) a high affinity DOTA analog which has previously shown high uptake in receptor specific tissues.

Both DOTA and DTPA conjugated bombesin analogs were radiolabeled with In-111 at high radiochemical purity (> 95%) and high specific activity (100 MBq/nmol for DOTA and 174 MBq/nmol for DTPA conjugated peptide). The specific activities for ^{111}In-labeled DTPA bombesin conjugates were higher than previously described (Zhang et al., 2004). For in vitro and in vivo comparisons in this work, the specific activity of the radiopeptides was adjusted to the same value.

To evaluate the levels of binding of the radiopeptides to bombesin receptors on different tumor cell lines, binding assays were performed with ^{111}In-DOTA-BEYG$_5$N on prostate (PC-3 and LNCaP) and breast (BT-474, MDA-MB-231 and T-47D) cancer cells. In accordance with literature data, in which [Tyr^4]BBN was used as ligand, both prostate cancer cells lines (Maddalena et al., 2009) and T-47D breast cancer cell line (Liu et al., 2009) demonstrated the presence of receptors. Although these published studies have shown bombesin receptors to be expressed in moderate levels on BT-474 and in low levels on MDA-MB-231 using [Tyr4]BBN (Liu et al., 2009), ^{111}In-DOTA-BEYG5N did not bind to these cell lines. This could possibly be due to differences in cell line source, culture and maintenance affecting the levels of expression of receptors on the cell surface.

Differences between the analysis of GRPR expression by Western Blot and radioligand binding assay were found in breast cancer tumor cells. Analysis of cell membranes by Western blot showed that MDA-MB-231 had a higher amount of receptor than BT-474 and T-47D, but the bombesin analog ^{111}In-DOTA-BEYG$_5$N bound only to T-47D in specific binding assay. The reason for this discrepancy is probably due to the fact that although Western blot

can show the presence of receptor protein, since the assay is carried out on lysed cell material, it cannot predict the availability of receptors to external ligands in intact cell studies. In order to fully understand the differences seen between protein expression and receptor binding, further studies using immunofluorescence to see where the receptors are located are warranted. An optimal bombesin agonist for tumor imaging and radionuclide therapy should have high and specific receptor binding followed by internalization. Therefore, we studied the saturation binding of ^{111}In-DOTA-BEYG$_5$N and ^{111}In-DTPA-BEYG$_5$N to those GRPR-expressing cell lines to which ^{111}In-DOTA-BEYG$_5$N had been seen to bind specifically i.e. PC-3, LNCaP and T-47D. Their internalization and externalization profiles on the highest GRPR expressing cell line, PC-3, were also studied. Both radiopeptides bind with high affinity to PC-3 and LNCaP prostate cancer cells as well as to the lower receptor-expressing breast cancer cell line, T-47D. However, the overall binding of ^{111}In-DOTA-BEYG$_5$N was seen to be two-fold higher to PC-3 and LNCaP cells than that of ^{111}In-DTPA-BEYG$_5$N. This cannot be attributed to affinity (the peptides have similar affinity for GRPR), however the higher binding of the DOTA-radiopeptide could possibly be due to differences in the overall charge of the chelator-radioisotope complexes. ^{111}In-DOTA complexes are uncharged while ^{111}In-DTPA complexes are negatively charged (Malmberg et al., 2012; Sabbah et al., 2007). This charge difference may cause the peptide to interact with the cell surface receptor in a different way providing a more or less stable peptide receptor complex. This is supported by the differences in the levels of internalization seen for the two peptides in PC3 cells with the negatively charged ^{111}In-DTPA-BEYG$_5$N showing lower internalization, although no differences were found between the externalization of the peptides. These results differ from previous literature data, which reported no difference in internalization of the DTPA (BZH1) and DOTA (BZH2) pan-bombesin analogs (Zhang et al., 2004), although this example is doubtless more complex due to binding to all three BN receptors. This supports the view that the influence of the chelator can vary from one bombesin peptide analog to another.

After performing the in vitro assays, the potential usefulness of^{111}In-DOTA-BEYG$_5$N and ^{111}In-DTPA-BEYG$_5$N for in vivo targeting and imaging of tumors expressing both high and low levels of GRPR was evaluated in the highest GRPR expressing cell lines, PC-3 and LNCaP and also compared to the previously published bombesin agonist BZH3. This agonist was included because of its high tumor uptake in preclinical studies of the ^{67}Ga-labeled compound at 4 h (6.47% ID/g in AR42J tumor) and also high pancreatic uptake (37.5% ID/g) (Schuhmacher et al., 2005). In our study of the ^{111}In-labeled BZH3, the tumor uptake was much reduced ($1.40 \pm 0.2\%$ ID/g and $1.50 \pm 0.4\%$ ID/g in PC3 and LNCaP tumors, respectively). Uptake in the pancreas was similarly reduced ($8.37 \pm 1.5\%$ ID/g and $11.14 \pm 3.1\%$ ID/g in PC3 and LNCaP tumor bearing mice, respectively). As predicted by saturation binding and internalization assays, the uptake in biodistribution studies of ^{111}In-DOTA-BEYG$_5$N in PC-3 and LNCaP tumors was higher than that of ^{111}In-DTPA-BEYG$_5$N. Moreover, PC-3 tumor uptake of both radiopeptides was significantly lower than ^{111}In-BZH3 (0.81 ± 0.1 and 0.49 ± 0.1 ID/g, respectively) but this result was not observed in LNCaP tumor.

The normal pancreas is the organ with the highest GRPR expression in mouse. Therefore, the tumor to pancreatic uptake ratio is of concern when comparing GRPR targeting peptides. Despite their lower PC-3 tumor uptake, tumor to pancreas ratio was higher for ^{111}In-DOTA-BEYG$_5$N and ^{111}In-DTPA-BEYG$_5$N than for ^{111}In-BZH3. These higher tumor to pancreatic ratios were also observed in LNCaP tumors. These results confirm the literature data which showed that there is not a direct relationship between tumor uptake and pancreatic uptake for bombesin analogs (Pujatti

et al., 2011) and these differences are probably due to variation in wash out of bombesin analogs from pancreas and tumor, which are greater for bombesin antagonists (Abiraj et al., 2011; Mansi et al., 2011).

The absolute tumor uptake of ^{111}In-BZH3, as well as pancreatic uptake, is much lower than previously described (Schuhmacher et al., 2005), and similar variation in results of comparative studies have been seen by the Rotterdam group (Schroeder et al., 2010) with as much reduction in tumor uptake as 16.2% ID/g down to 3% ID/g seen for Demobesin 1. As suggested, the variation in mouse strain, PC-3 tumor cells (source, passage number, culture conditions), tumor size and vascularization may be factors that determine uptake of radioactivity resulting in variable outcomes (Schroeder et al., 2010). For this reason BZH3 was used as a standard in order to avoid the influence of these factors in in vivo studies, which could compromise the comparison.

NanoSPECT/CT imaging showed that visualization of PC-3 and LNCaP tumors is possible with ^{111}In-BZH3, ^{111}In-DOTA-BEYG$_5$N and ^{111}In-DTPA-BEYG$_5$N. Quantification of uptake in tumor and muscle allowed calculation of tumor to muscle ratios, which ideally should be high and increase over time, suggesting high retention in tumor and declining background activity. PC-3 and LNCaP tumor to muscle ratios were high for the three radiopeptides 1 and 4 h p.i., but an increase was only observed in PC-3 tumor to muscle ratio of ^{111}In-DOTA-BEYG$_5$N. These data indicate that the three peptides have fast blood clearance, which reduce the radiopeptides in circulation and non-target tissues to a minimum before 1 h p.i.

Another important factor to consider in evaluation of a radiopeptide for tumor imaging is its metabolic stability in blood and tumor. The in vivo metabolic stability in blood of both peptides is low when compared to their in vitro stability and to in vivo stability of some bombesin derivatives previously described (between 10% and 65% of intact radiopeptide 5 min p.i., depending on the peptide) (Schroeder et al., 2010) and very low amounts of ^{111}In-DOTA-BEYG$_5$N and ^{111}In-DTPA-BEYG$_5$N remain intact in circulation 5 min p.i.. However, the studied bombesin analogs could target the tumor and remained stable in tumor cells, especially ^{111}In-DOTA-BEYG$_5$N, which had tumor stability comparable to that of ^{111}In-BZH3. These results suggest that the peptides undergo very fast blood clearance that allows tumor targeting before the complete degradation of the bombesin analogs by serum enzymes.

Biodistribution studies and NanoSPECT/CT imaging also showed that it is not always possible to predict the number of active receptors on tumor cells in vivo. One would have predicted higher tumor uptake for PC-3 cells as the receptor density is higher, however the opposite effect was seen. This may be due to the highly vascular nature of LNCaP tumors with a larger component of tumor uptake being attributable to increased vascularity for the LNCaP model. Also, as previously demonstrated, LNCaP tumor characteristically exhibits extravasation of blood (ecchymosis), which results in blue, purple, or red patches across the tumor surface. This blood pool seeps into the tumor surround (Maddalena et al., 2009) and could increase the peptide binding in vivo by increasing its time of contact with tumor cells surface. Nevertheless, in vivo blocking studies in the PC3 tumor model showed that the uptake of the most promising of the two analogs (^{111}In-DOTA-BEYG$_5$N) is receptor specific and can be competed out by co-administration of unlabeled peptide.

5. Conclusions

Our results showed that different in vitro and in vivo methods should be applied to preclinical comparison of labeled peptides. Each method provides useful information about the labeled

peptide and the analysis of their entire results allows us to draw conclusions in a more reliable way. Taking all the methods studied together, we conclude that [Tyr–Gly$_5$, Nle^{14}]-BBN(6–14) can be a useful tool for GRPR positive tumor targeting and imaging. The DOTA-conjugated analog is superior to its DTPA-conjugated counterpart in terms of tumor cell binding and internalisation as well as in vivo stability in blood and tumor.

References

Abiraj, K., Mansi, R., Tamma, M.L., Fani, M., Forrer, F., Nicolas, G., Cescato, R., Reubi, J. C., Maecke, H.R., 2011. Bombesin antagonist-based radioligands for translational nuclear imaging of gastrin-releasing peptide receptor-positive tumors. J. Nucl. Med. 52, 1970–1978.

Beer, M., Montani, M., Gerhardt, J., Wild, P.J., Hany, T.F., Hermanns, T., Muntener, M., Kristiansen, G., 2012. Profiling gastrin-releasing peptide receptor in prostate tissues: clinical implications and molecular correlates. Prostate 72, 318–325.

Breeman, W.A., de Jong, M., Erion, J.L., Bugaj, J.E., Srinivasan, A., Bernard, B.F., Kwekkeboom, D.J., Visser, T.J., Krenning, E.P., 2002. Preclinical comparison of (111)In-labeled DTPA- or DOTA-bombesin analogs for receptor-targeted scintigraphy and radionuclide therapy. J. Nucl. Med. 43, 1650–1656.

Csizmadia, F., Tsantili-Kakoulidou, A., Panderi, I., Darvas, F., 1997. Prediction of distribution coefficient from structure. 1. Estimation method. J. Pharm. Sci. 86, 865–871.

de Visser, M., Bernard, H.F., Erion, J.L., Schmidt, M.A., Srinivasan, A., Waser, B., Reubi, J.C., Krenning, E.P., de Jong, M., 2007. Novel ^{111}In-labelled bombesin analogues for molecular imaging of prostate tumours. Eur. J. Nucl. Med. Mol. Imaging 34, 1228–1238.

Fani, M., Del Pozzo, L., Abiraj, K., Mansi, R., Tamma, M.L., Cescato, R., Waser, B., Weber, W.A., Reubi, J.C., Maecke, H.R., 2011. PET of somatostatin receptor-positive tumors using 64Cu- and 68Ga-somatostatin antagonists: the chelate makes the difference. J. Nucl. Med. 52, 1110–1118.

Fleischmann, A., Waser, B., Reubi, J.C., 2009. High expression of gastrin-releasing peptide receptors in the vascular bed of urinary tract cancers: promising candidates for vascular targeting applications. Endocr. Relat. Cancer 16, 623–633.

Gourni, E., Mansi, R., Jamous, M., Waser, B., Smerling, C., Burian, A., Buchegger, F., Reubi, J.C., Maecke, H.R., 2014. N-terminal modifications improve the receptor affinity and pharmacokinetics of radiolabeled peptidic gastrin-releasing peptide receptor antagonists: examples of 68Ga- and 64Cu-labeled peptides for PET imaging. J. Nucl. Med. 55 (10), 1719–1725.

Jamous, M., Tamma, M.L., Gourni, E., Waser, B., Reubi, J.C., Maecke, H.R., Mansi, R., 2014. PEG spacers of different length influence the biological profile of bombesin-based radiolabeled antagonists. Nucl. Med. Biol. 41, 464–470.

Lantry, L.E., Cappelletti, E., Maddalena, M.E., Fox, J.S., Feng, W., Chen, J., Thomas, R., Eaton, S.M., Bogdan, N.J., Arunachalam, T., Raju, N., Metcalfe, E.C., Lattuada, L., Linder, K.E., Swenson, R.E., Tweedle, M.F., Nunn, A.D., 2006. 177Lu-AMBA: synthesis and characterization of a selective 177Lu-labeled GRP-R agonist for systemic radiotherapy of prostate cancer. J. Nucl. Med. 47, 1144–1152.

Lane, S.R., Nanda, P., Rold, T.L., Sieckman, G.L., Figueroa, S.D., Hoffman, T.J., Jurisson, S.S., Smith, C.J., 2010. Optimization, biological evaluation and microPET imaging of copper-64-labeled bombesin agonists, [64Cu–NO2A–(X)-BBN(7–14)NH2], in a prostate tumor xenografted mouse model. Nucl. Med. Biol. 37, 751–761.

Laverman, P., Sosabowski, J.K., Boerman, O.C., Oyen, W.J., 2012. Radiolabelled peptides for oncological diagnosis. Eur. J. Nucl. Med. Mol. Imaging 39 (Suppl. 1), S78–S92.

Liu, C., Pierce 2nd, L.A., Alessio, A.M., Kinahan, P.E., 2009. The impact of respiratory motion on tumor quantification and delineation in static PET/CT imaging. Phys. Med. Biol. 54, 7345–7362.

Liu, Y., Hu, X., Liu, H., Bu, L., Ma, X., Cheng, K., Li, J., Tian, M., Zhang, H., Cheng, Z., 2013. A comparative study of radiolabeled bombesin analogs for the PET imaging of prostate cancer. J. Nucl. Med. 54, 2132–2138.

Maina, T., Nock, B.A., Zhang, H., Nikolopoulou, A., Waser, B., Reubi, J.C., Maecke, H.R., 2005. Species differences of bombesin analog interactions with GRP-R define the choice of animal models in the development of GRP-R-targeting drugs. J. Nucl. Med. 46, 823–830.

Markwalder, R., Reubi, J.C., 1999. Gastrin-releasing peptide receptors in the human prostate: relation to neoplastic transformation. Cancer Res. 59, 1152–1159.

Mantey, S.A., Weber, H.C., Sainz, E., Akeson, M., Ryan, R.R., Pradhan, T.K., Searles, R. P., Spindel, E.R., Battey, J.F., Coy, D.H., Jensen, R.T., 1997. Discovery of a high affinity radioligand for the human orphan receptor, bombesin receptor subtype 3, which demonstrates that it has a unique pharmacology compared with other mammalian bombesin receptors. J. Biol. Chem. 272, 26062–26071.

Mansi, R., Wang, X., Forrer, F., Waser, B., Cescato, R., Graham, K., Borkowski, S., Reubi, J.C., Maecke, H.R., 2011. Development of a potent DOTA-conjugated bombesin antagonist for targeting GRPr-positive tumours. Eur. J. Nucl. Med. Mol. Imaging 38, 97–107.

Marsouvanidis, P.J., Maina, T., Sallegger, W., Krenning, E.P., de Jong, M., Nock, B.A., 2013. Tumor diagnosis with new ^{111}In-radioligands based on truncated human gastrin releasing peptide sequences: synthesis and preclinical comparison. J. Med. Chem. 56, 8579–8587.

Maddalena, M.E., Fox, J., Chen, J., Feng, W., Cagnolini, A., Linder, K.E., Tweedle, M.F., Nunn, A.D., Lantry, L.E., 2009. 177Lu-AMBA biodistribution, radiotherapeutic efficacy, imaging, and autoradiography in prostate cancer models with low GRP-R expression. J. Nucl. Med. 50, 2017–2024.

Malmberg, J., Perols, A., Varasteh, Z., Altai, M., Braun, A., Sandstrom, M., Garske, U., Tolmachev, V., Orlova, A., Karlstrom, A.E., 2012. Comparative evaluation of synthetic anti-HER2 Affibody molecules site-specifically labelled with ^{111}In using N-terminal DOTA, NOTA and NODAGA chelators in mice bearing prostate cancer xenografts. Eur. J. Nucl. Med. Mol. Imaging 39, 481–492.

Okarvi, S.M., Jammaz, I.A., 2012. Preparation and evaluation of bombesin peptide derivatives as potential tumor imaging agents: effects of structure and composition of amino acid sequence on in vitro and in vivo characteristics. Nucl. Med. Biol. 39, 795–804.

Ocak, M., Helbok, A., Rangger, C., Peitl, P.K., Nock, B.A., Morelli, G., Eek, A., Sosabowski, J.K., Breeman, W.A., Reubi, J.C., Decristoforo, C., 2011. Comparison of biological stability and metabolism of CCK2 receptor targeting peptides, a collaborative project under COST BM0607. Eur. J. Nucl. Med. Mol. Imaging 38, 1426–1435.

Pradhan, T.K., Katsuno, T., Taylor, J.E., Kim, S.H., Ryan, R.R., Mantey, S.A., Donohue, P. J., Weber, H.C., Sainz, E., Battey, J.F., Coy, D.H., Jensen, R.T., 1998. Identification of a unique ligand which has high affinity for all four bombesin receptor subtypes. Eur. J. Pharmacol. 343, 275–287.

Pujatti, P.B., Santos, J.S., Couto, R.M., Melero, L.T., Suzuki, M.F., Soares, C.R., Grallert, S.R., Mengatti, J., De Araujo, E.B., 2011. Novel series of (177)Lu-labeled bombesin derivatives with amino acidic spacers for selective targeting of human PC-3 prostate tumor cells. Q. J. Nucl. Med. Mol. Imaging 55, 310–323.

Reubi, J.C., Wenger, S., Schmuckli-Maurer, J., Schaer, J.C., Gugger, M., 2002. Bombesin receptor subtypes in human cancers: detection with the universal radioligand (125)I-[D-TYR(6), beta-ALA(11), PHE(13), NLE(14)] bombesin(6-14). Clin. Cancer Res. 8, 1139–1146.

Reubi, C., Gugger, M., Waser, B., 2002. Co-expressed peptide receptors in breast cancer as a molecular basis for in vivo multireceptor tumour targeting. Eur. J. Nucl. Med. Mol. Imaging 29, 855–862.

Reubi, J.C., 2003. Peptide receptors as molecular targets for cancer diagnosis and therapy. Endocr. Rev. 24, 389–427.

Smith, C.J., Volkert, W.A., Hoffman, T.J., 2005. Radiolabeled peptide conjugates for targeting of the bombesin receptor superfamily subtypes. Nucl. Med. Biol. 32, 733–740.

Schuhmacher, J., Zhang, H., Doll, J., Macke, H.R., Matys, R., Hauser, H., Henze, M., Haberkorn, U., Eisenhut, M., 2005. GRP receptor-targeted PET of a rat pancreas carcinoma xenograft in nude mice with a 68Ga-labeled bombesin(6–14) analog. J. Nucl. Med. 46, 691–699.

Sosabowski, J.K., Matzow, T., Foster, J.M., Finucane, C., Ellison, D., Watson, S.A., Mather, S.J., 2009. Targeting of CCK-2 receptor-expressing tumors using a radiolabeled divalent gastrin peptide. J. Nucl. Med. 50, 2082–2089.

Sabbah, E.N., Kadouche, J., Ellison, D., Finucane, C., Decaudin, D., Mather, S.J., 2007. In vitro and in vivo comparison of DTPA- and DOTA-conjugated antiferritin monoclonal antibody for imaging and therapy of pancreatic cancer. Nucl. Med. Biol. 34, 293–304.

Schroeder, R.P., Muller, C., Reneman, S., Melis, M.L., Breeman, W.A., de Blois, E., Bangma, C.H., Krenning, E.P., van Weerden, W.M., de Jong, M., 2010. A standardised study to compare prostate cancer targeting efficacy of five radiolabelled bombesin analogues. Eur. J. Nucl. Med. Mol. Imaging 37, 1386–1396.

Viswanadhan, V.N., Ghose, A.K., Revankar, G.R., Robins, R.K., 1989. Atomic physicochemical parameters for three dimensional structure directed quantitative structure-activity relationships. 4. Additional parameters for hydrophobic and dispersive interactions and their application for an automated superposition of certain naturally occurring nucleoside antibiotics. J. Chem. Inf. Comput. Sci. 29, 163–172.

Wild, D., Frischknecht, M., Zhang, H., Morgenstern, A., Bruchertseifer, F., Boisclair, J., Provencher-Bolliger, A., Reubi, J.C., Maecke, H.R., 2011. Alpha- versus betaparticle radiopeptide therapy in a human prostate cancer model (213Bi-DOTA-PESIN and 213Bi-AMBA versus 177Lu-DOTA-PESIN). Cancer Res. 71, 1009–1018.

Zhang, H., Chen, J., Waldherr, C., Hinni, K., Waser, B., Reubi, J.C., Maecke, H.R., 2004. Synthesis and evaluation of bombesin derivatives on the basis of pan-bombesin peptides labeled with indium-111, lutetium-177, and yttrium-90 for targeting bombesin receptor-expressing tumors. Cancer Res. 64, 6707–6715.